GEOCHRONOMETRIA 51 (2024) 192337
DOI 10.20858/geochr/192337

Available online at https://www.geochronometria.com/

RESPONSE OF RADIAL GROWTH OF *P. SYLVESTRIS VAR. MONGOLICA* (*P. SYLVESTRIS*) AND *LARIX GMELINII* (*RUPR.*) *KUZEN* (*L. GMELINII*) TO EXTREME CLIMATE AND THEIR FUTURE GROWTH TRENDS IN THE DAXING'ANLING MOUNTAINS, NORTHEAST CHINA

RUXIANGULI·ABUDUREHEMAN[1, 2, 3], TONGWEN ZHANG[2, 3, 4], SHULONG YU[1, 2, 3], RUIBO ZHANG[1, 2, 3], HUAMING SHANG[1, 2, 3], KEXIANG LIU[1, 2, 3], XIAOXIA GOU[1, 2, 3], DONG GUO[1, 2, 3] and YUJIANG YUAN[1, 2, 3]

[1]Institute of Desert Meteorology, China Meteorological Administration, Urumqi 830002, China
[2]Key Laboratory of Tree-ring Physical and Chemical Research of China Meteorological Administration, Urumqi 830002, China
[3]Key Laboratory of Tree-ring Ecology of Uygur Autonomous Region, Urumqi 830002, China
[4]Xinjiang Climate Center, Urumqi 830002, China

Received 1 April 2024 Accepted 14 August 2024

Abstract
The Daxing'anling Mountains are vulnerable to extreme weather and ecological degradation. Forests in this region have been substantially affected by extreme events; however, the pattern of future forest change remains uncertain. To determine the trends and reasons for extreme climate change, reanalysis data were used to assess the potential forest degradation resulting from future extreme climate events. Using tree-ring width chronologies of *Pinus sylvestris var. mongolica* (1952–2015) and *Larix gmelinii (Rupr.) Kuzen* (1962–2015), we performed a comparative analysis of the relationships between radial growth of these two tree species and extreme indices based on Pearson correlations. The functions between extreme climate and tree ring width were then used in the LASSO algorithm. Using the CMIP6 models under the intermediate emission scenario (SSP2-4.5), we projected the tree ring width of the two species from 2015 to 2100 using calibrated meteorological fields. The tree-ring chronologies of both species were correlated negatively with extreme warm temperature indices and positively with extreme precipitation indices. *P. sylvestris* responded more significantly to extremely high temperature indices and precipitation, with a certain lag effect. *L. gmelinii* responded significantly to extremely cold temperature indices. Tree species specificity may explain why the two species show different growth–climate relationships. The growth of *P. sylvestris* may decrease during extreme climate change conditions, whereas the effect on *L. gmelinii* future growth is not significant. The predicted growth series in the 2015–2100 period showed that three abnormally high values, six abnormally low values, and one extreme abnormally low value occurred in *P. sylvestris*, whereas there were two extreme abnormally low values, four abnormally low values, and four abnormally high values in *L. gmelinii*. Our findings can help predict the resilience and sustainability of forest ecosystems in the face of extreme climate change and contribute to forest management strategies.

Keywords
Daxing'anling, Extreme climate events, *P. sylvestris*, *L. gmelinii*, Tree-ring width, Future growth trends

Corresponding author: T. Zhang
e-mail: zhangtw@idm.cn

ISSN 1897-1695 (online), 1733-8387 (print)

1. Introduction

According to the IPCC Sixth Assessment Report, further climate warming is expected to lead to more frequent and severe extreme weather events, including heat waves, heavy precipitation, droughts, and typhoons. These events pose a substantial threat to human societies and natural ecosystems (IPCC, 2021). To address this challenge, several studies have used climate models to assess the regional variability of precipitation and temperature extremes (Chen *et al.*, 2020; Zhu *et al.*, 2021; Thackeray *et al.*, 2022; Zhang *et al.*, 2023b), with most reporting that future temperature extremes with greater warming are expected at high- and mid-latitudes compared with low-latitudes. Therefore, it is of paramount importance to gain a thorough understanding of the characteristics of extreme climate events and their impacts on regional ecological environments.

Forests, as the largest terrestrial ecosystem on Earth, play an irreplaceable role in maintaining the ecological balance of the planet and the sustainable development of human society (Reichstein *et al.*, 2007; Allen *et al.*, 2010). However, extreme climatic events, induced by climate warming, pose a significant threat to forest succession and tree growth, potentially leading to forest decline and mortality (Holm *et al.*, 2023; Roshani *et al.*, 2022). Extreme events typically lead to stronger responses and shorter response times than normal climatic events (Kreyling *et al.*, 2011). In the boreal forests of Siberia, the concurrent occurrence of anomalous warming and drought has destabilized forest ecosystems, causing the northern timberline to advance into previously frigid tundra regions (Esper and Schweingruber, 2004). Moreover, the record-breaking heatwave in Europe during the summer of 2003 precipitated a 30% decrease in the aggregate primary productivity of forest ecosystems (Ciais *et al.*, 2005). Extreme precipitation events, exemplified by torrential rain and flooding, can trigger soil erosion, river sedimentation, forest waterlogging, and hypoxia, all of which detrimentally influence tree growth and forest ecosystem health (Sanginés de Cárcer *et al.*, 2017; Dannenberg *et al.*, 2021; O'Donnell *et al.*, 2021). In addition, differences between tree species in the same habitat can lead to a divergence in climate responses. For instance, conifer species' drought resilience is contingent on leaf longevity during drought conditions, whereas broadleaf species counter drought adversity by enhancing water uptake and storage through more extensive root systems (Song *et al.*, 2022; Kulha *et al.*, 2023; Zhang *et al.*, 2023a). Evergreen and deciduous plants also manifest distinct adaptive strategies towards freezing temperatures—evergreens exhibit cold tolerance, while deciduous species exhibit resistance to hydrodynamic impediments and higher water transport efficiency. Zang *et al.* (2014) conducted a comparative analysis of drought tolerance among three prevalent temperate European forest species: *Norway spruce*, *silver fir* and *common beech*, identifying *Norway spruce* as being particularly drought-tolerant. Li *et al.* (2020) investigated the radial growth response to climate variability in the central Loess Plateau using *Pinus sylvestris* and *Fagus sylvatica*, discovering that a humid milieu is conducive to *P. sylvestris* growth. Collectively, these studies showed that tree species specificity significantly modulates their responses to extreme climatic events, offering critical insights for forest management and ecosystem revitalization.

The Daxing'anling Mountains are an important mountain range in northeast China. Because of the interannual instability of the East Asian monsoon, frequent climate extremes, particularly high temperature or drought events, have a substantial impact on forest ecosystems in the region (Jiang *et al.*, 2016). In 1987, an exceptional drought triggered a catastrophic forest fire in Daxing'anling, devastating an area exceeding 1 million ha of forest, and causing significant damage to the forest ecosystem. Frequent climate extremes in the future will cause a decline in the growth of *Larix gmelinii* in the Daxing'anling area, resulting in a gradual northward shift in its distribution that potentially extends beyond China (Leng *et al.*, 2007). Nevertheless, the impact of the changing complexity of extreme indices on different tree growth and future trends remain uncertain. Tree rings record past extreme climates with high accuracy and annual resolution, making them an important way to study the relationship between tree growth and extreme climatic events (Izworska *et al.*, 2023). Despite this, current research on tree ring largely focuses on conventional climate responses and climate reconstruction, leaving a significant gap in our understanding of the diverse growth responses of trees to climate extremes and their future trends. Furthermore, there is a lack of comprehensive approaches to assess tree growth in the Daxing'anling Mountains using the latest Coupled Model Comparison Program Phase 6 (CMIP6) global climate model projections. This gap hinders the prediction of future forest dynamics and the implementation of effective responses to mitigate the impacts of extreme weather events on forest ecosystem functioning and the terrestrial carbon balance in the Daxing'anling Mountains. Given the increasing frequency of extreme events in Daxing'anling, there is an urgent need for a deeper understanding and prediction of the impacts of extreme climatic events on the growth of different tree species and how these impacts will shape future growth and distribution. This is essential for the development of forest management and climate change adaptation strategies in Daxing'anling. To investigate the scientific problems outlined above, we compared and analyzed the correlations between extreme climatic conditions and the tree-ring width chronologies of two tree species: *P. sylvestris var. mongolica* (*P. sylvestris*) and *L. gmelinii (Rupr.) Kuzen* (*L. gmelinii*) and identified the major extreme climatic factors affecting the radial growth of both species. Additionally, we used the Lasso regression (LASSO) algorithm to explore the complex relationships between extreme climate and tree growth and we developed functions to quantify tree-ring width during climate

change. Finally, on the basis of the model fitting results and the CMIP6 model, which represents climate projections under the greenhouse gas emission scenario (SSP2-4.5) in the latest dataset, the future growth trends of *P. sylvestris* and *L. gmelinii* were predicted. These results may improve our responses to and reduce the impact of climate extremes on forest ecosystems.

2. Materials and methods

2.1 Study area

The sampling site was located in the Ta He area (52°22′ N, 124°45′ E) north of the Daxing'anling Mountains, bounded by the middle reaches of the Huma River (Gao *et al.*, 2019). Owing to the difference in altitude and geographical location, Daxing'anling exhibits a distinct continental climate. Extreme climate events such as severe cold and heavy snowfall are more common in winter, whereas summer can lead to heat waves and heavy rainfall. The Daxing'anling Mountains are one of the most important forest ecosystems in China, covered by large areas of virgin forest. The predominant tree species at the site are *P. sylvestris* and *L. gmelinii* (Li *et al.*, 1993). These two species are known for their resistance to cold and drought, as well as their ability to adapt to climatic conditions.

2.2 Sample collection and tree-ring width chronology development

The tree species sampled in this paper were *P. sylvestris* (52°22'14.10" N, 124°45'8.13" E) and *L. gmelinii* (52°22'24.9" N, 124°46'53.00" E), and there was no obvious impact of human activities in the sampling area (**Fig. 1**). Following the requirements of the tree-ring standards, two sample cores were drilled from each tree at 1.3 m height in two crosswise directions using a growth cone with an inner diameter of 10 mm. In this study, cores from 21 *P. sylvestris* (42 cores) and 26 *L. gmelinii* (52 cores) were collected. The collection information is shown in **Table 1**.

The cores were brought back to the laboratory for air-drying. They were glued and fixed in wooden grooves with white latex, and sandpapered step by step until they showed a clear and recognizable annual ring boundary (Fritts, 1976). Afterward, the width of the rings was measured using a LINTAB 5 tree-rotor meter with an accuracy of 0.01 mm (Grissino-Mayer, 2001). All cores were rigorously cross-dated and quality-controlled using the

Table 1. *Information about the sampling sites.*

Tree species	Site code	Latitude (N)	Longitude (E)	Elevation (m)	Number of trees (cores)	Maximum tree age
P. sylvestris	YAZ	52°22'14.10"	124°45'8.13"	426	21(42)	1952–2015
L. gmelinii	YAL	52°22'24.90"	124°46'53.00"	381	26(52)	1962–2015

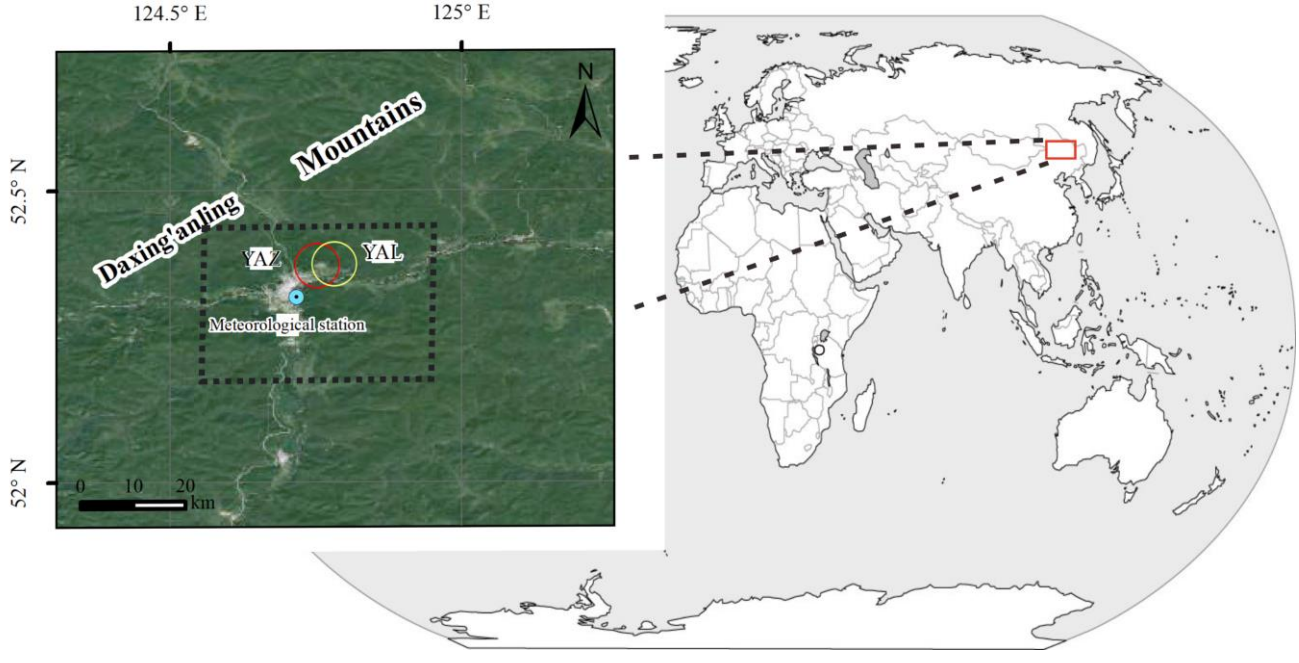

Fig. 1. *Location of the study area and the sampling sites (YAZ, YAL).*

COFECHA procedure to achieve an overall high level of correlation. The ARSTAN procedure was used to detrend and build a tree-ring chronology (Cook, 1985). In this study, a single detrending procedure using a negative exponential function (a conservative function applied to tree-ring measurement) eliminated age- and size-related variation in tree-ring width to create a standardized chronology, which was used as the tree-ring width data for the subsequent analyses in our study (Wigley *et al.*, 1984). The standardized chronology contained common variations between individual tree core series and retained low to high-frequency common variations.

2.3 Meteorological data

The daily maximum temperature, minimum temperature, and precipitation data used in this study were acquired from the meteorological station of Tahe, Heilongjiang (52°19' N, 124°43' E). The timescale used was 1972–2015, because the chronological sampling data ended in 2015. This study selected 27 extreme climate indices proposed by the CCI/CLIVAR/JCOMM Expert Team on Climate Change Detection and Indices (http://etccdi.pacificclimate.org), including seven extreme high-temperature indices, seven extreme low-temperature indices, 11 extreme precipitation indices and other indices (**Table 2**). The extreme precipitation index was divided into a frequency index and a class index for better observation and analysis (Bonsal *et al.*, 2001; Ali *et al.*, 2019). Extreme indices were calculated, and the quality was rigorously determined using RClimDex V1.0. To determine the reasons for extreme climate change, we analyzed the monthly mean geopotential height and wind fields at 850 hPa from 1972 to 2015 using NCEP/NCAR reanalysis data with a resolution of 2.5°×2.5° (https://psl.noaa.gov/data/gridded/data.ncep.reanalysis.pressure.html). In addition, the forecast daily value data from 2015–2100 were obtained from the CMIP6 model, which was downloaded from the NASA Earth Exchange/Global Daily Downscaled Projections with a resolution of 0.25° (~25 km × 25 km). To minimize the discrepancies between simulated data from

Table 2. *Extreme climate index.*

Classify	Index	Descriptive name	Definition	Units
Extreme high temperature indices	TXx	Warmest daily Tmax	Seasonal/annual maximum value of daily maximum temperature	°C
	TXn	Coldest daily Tmax	Seasonal/annual minimum value of daily maximum temperature	°C
	TX90p	Warm days	Days (or fraction of time) when daily maximum temperature >90th percentile	d
	TN90p	Warm nights	Days (or fraction of time) when daily minimum temperature >90th percentile	d
	WSDI	Warm spell duration indicator	Days maximum temperature (TX) >90% for at least 6 consecutive days every year	d
	SU25	Summer days	Days with daily maximum temperature (TX) >25°C	d
	TR20	Tropical nights	Frequency of daily minimum temperature >20°C	d
Extreme low temperature indices	TNx	Warmest daily Tmin	Seasonal/annual maximum value of daily minimum temperature	°C
	TNn	Coldest daily Tmin	Seasonal/annual minimum value of daily minimum temperature	°C
	TX10p	Cold days	Days (or fraction of time) when daily maximum temperature	d
	TN10p	Cold nights	Days (or fraction of time) when daily minimum temperature	d
	CSDI	Cold spell duration indicator	Days minimum temperature (TN) <10% quantile for at least 6 consecutive days per year	d
	FD0	Frost days	Frequency of daily minimum temperature <0°C	d
	ID0	Icing days	Days with daily maximum temperature (TX) <0°C	d
Other temperature indices	Temp	Average temperature	The average monthly and annual temperature	°C
	GSL	Growing season length	At least 6 consecutive days with daily average temperature >5°C on the first day and 6 consecutive days	d
	DTR	Daily temperature range	The diurnal between the maximum temperature (TX) and the minimum temperature (TN) of the month and year	°C
Precipitation frequency index	R10	Number of heavy precipitation days	Days with daily precipitation ≥10mm	d
	R20	Number of very heavy precipitation days	Days with daily precipitation ≥20mm	d
	R25	Number of very heaviest precipitation days	Days with daily precipitation ≥25mm	d
	CDD	Consecutive dry days	Maximum number of consecutive dry days	d
	CWD	Consecutive wet days	Maximum number of consecutive wet days	d
Precipitation class index	RX1day	Wettest day	Maximum 1-day precipitation	mm
	Rx5day	Wettest consecutive five days	Maximum of consecutive 5-day precipitation	mm
	R95p	Very wet days precipitation	Amount of precipitation from days >95%	mm
	R99p	Extremely wet day precipitation	Amount of precipitation from days >99%	mm
	PRCPTOT	Annual precipitation	Daily precipitation > 1mm annual cumulative amount	mm
	SDII	Simple daily intensity index	Ratio of annual total precipitation to the number of wet days (≥1 mm)	mm/day

different models, all model data employed the daily scale from the r1i1p1 series. Moreover, to effectively reduce the uncertainty in climate simulations, a weighted average method was used to aggregate six climate models from CMIP6 (BCC-CSM2-MR, CMCC-CM2-SR5, GFDL-CM4, GISS-E2-1-G, MPI-ESM1-2-IR, and TaiESM1). Studies have indicated that these models exhibit superior fitting performance for predicting temperature and precipitation in northeast China (Wang *et al.*, 2021; He *et al.*, 2022) (https://cds.nccs.nasa.gov/nex-gddp). For this study, we only used the SSP2-4.5 scenario because in examining the dynamic response stability relationship between tree rings and extreme climate factors, we observed a stable response. This suggests that under future climate change, the response of extreme climate factors to tree growth will generally follow past patterns. SSP2-4.5 scenario followed the historical pattern more closely than other emission scenarios (Wang *et al.*, 2023). This provided us with a relatively reliable baseline for predicting the relationship between future tree growth and climate response.

2.4 Statistical analysis

To examine the impact of extreme climate change on tree growth trends in a particular area, a linear regression model was used to estimate trends in extreme climate indices and standardized width chronologies. Additionally, a correlation analysis was conducted to assess the climatic signals embedded in the tree-ring chronologies. Owing to the strong biological lag effect, monthly extreme climate data from August of the previous year to October of the current year were analyzed to investigate the influence of climatic factors on the variation in tree-ring width of the two species. To speculate whether the relationship between the growth and climate in the past was within the range of conditions expected in the future, we also used sliding correlation analysis to investigate the long-term dynamics of tree-ring width in relation to extreme climatic factors for the two tree species. A fixed interval of 30 years was chosen to vary the start and end years of the analyzed series.

LASSO regression is commonly used to estimate data with complex collinearity among independent variables. The algorithm tends to shrink the coefficients of unimportant features to zero, effectively reducing dimensionality and improving the ability of the model for generalization. Generalized cross-validation was used to verify and select the penalty coefficients and parameters of the independent variables, resulting in a refined model (Frost and Amos, 2017). This is an efficient approach to obtaining a more predictive model (Ribbing *et al.*, 2007). The performance error of the model was quantified using mean square error (MSE). The extreme climate indices used in this study were calculated from daily maximum and minimum temperatures, and daily precipitation. There was high collinearity among the indices. Therefore, when fitting and forecasting the tree-ring width chronology based on the monthly data of each climate index, LASSO regression was used to screen and estimate the climatic factors and then forecast. The LASSO model parameters were adjusted to fit the chronological sequence of radial growth of the two species based on the climatic factors and their corresponding parameters after fitting and then combined with the future climate change prediction data under the SSP2.4-5 scenario to predict the radial growth of the two tree species.

3. Results

3.1 Extreme climate variation

Fig. 2 illustrates the temporal variation in mean annual extreme climatic events north of Daxing'anling from 1972 to 2015. The extreme temperature indices, including the annual minima of the daily maximum temperature (TXn), warm days (TX90p), warm nights (TN90p), warm spell duration indicator (WSDI), summer days (SU25), and diurnal temperature range (DTR), showed a significant increasing trend. Conversely, cold indices, such as icing days (ID0) and cold days (TX10p) showed significantly decreasing trends. In contrast, no significant change was observed in the extreme precipitation indices. Therefore, we concluded that, over the past 44 years, the probability of extreme warm temperature events has increased, whereas the probability of extreme cold temperature events has decreased north of Daxing'anling.

3.2 Tree-ring chronologies of the two tree species

The growth patterns of *P. sylvestris* and *L. gmelinii* were strongly correlated ($r = 0.518$, $p < 0.001$). High-frequency variations in growth patterns were also significantly correlated ($r = 0.649$, $p < 0.001$). This finding suggests that the two species exhibited similar high-frequency growth variations to some extent. The growth of the two species showed different rates of increase from 1952/1962 to 1988 (**Fig. 3**). The trends for *P. sylvestris* and *L. gmelinii* were statistically significant ($p < 0.01$) and increased at rates of 0.057 and 0.363 per decade, respectively.

Table 3 shows the statistical characteristics of *P. sylvestris* and *L. gmelinii* chronologies. The expressed population signals exceeded 0.85, indicating high chrono-

Table 3. *Statistical characteristics of* P. sylvestris *and* L. gmelinii *standard chronologies.*

Species	TS	EPS	MS	SD	MCC	AC1
P. sylvestris	1962–2015	0.982	0.193	0.238	0.609	0.595
L. gmelinii	1970–2015	0.977	0.254	0.350	0.518	0.349

Notes: TS (SSS > 0.85)-Time span, EPS-Expressed population signa, MS-Mean sensitivity, SD-Standard deviation, MCC-Mean correlation coefficients among all series, AC1-First order auto-correlation.

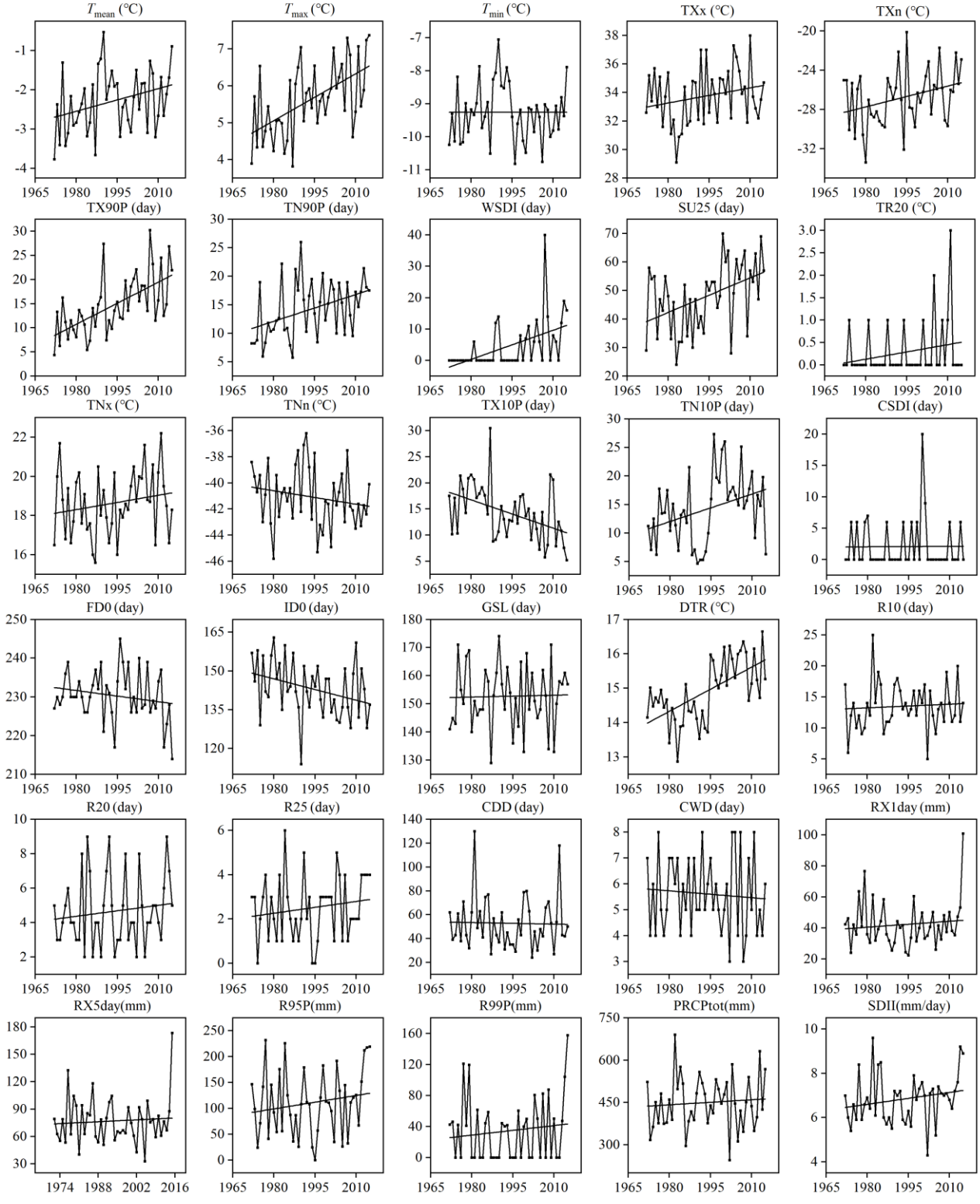

Fig. 2. *Interannual variation trends of extreme climate in the Daxing'anling Mountains during 1972–2015.*

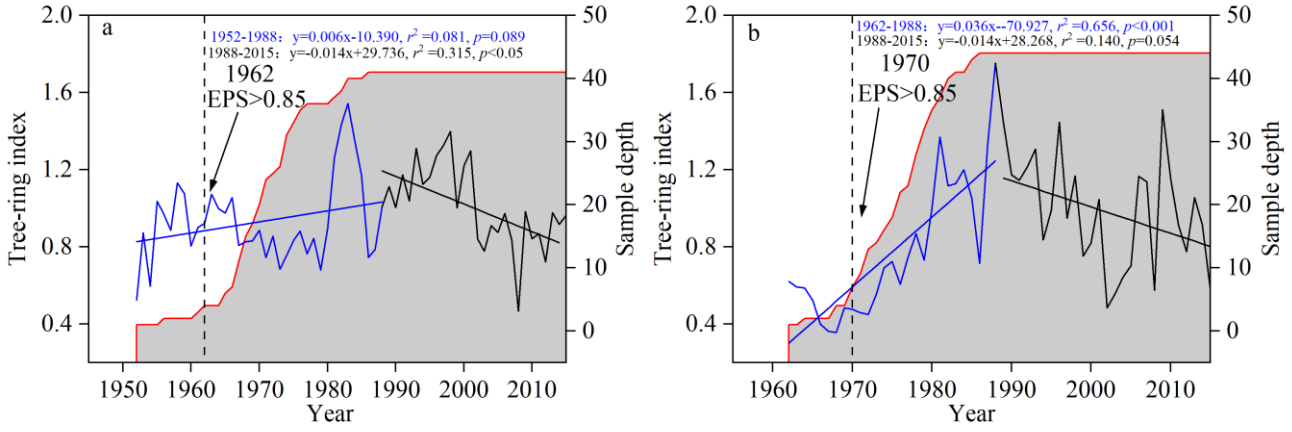

Fig. 3. *The standard chronologies and the corresponding sample depth of the* P. sylvestris *and* L. gmelinii.

logical quality. The chronologies of the two species were found to contain reasonable climate information based on mean sensitivity and standard deviation. The first-order autocorrelation of the *P. sylvestris* chronology was greater than that of *L. gmelinii*, indicating that climate change in the previous year had a greater impact on the tree-ring width of *P. sylvestris*. All these statistical values showed that the chronologies of the two species had a strong signal strength for research on climatic change.

3.3 Relationship between tree radial growth and extreme climate

The growth of the two species in response to extreme climate indices varied annually and monthly. *P. sylvestris* showed a positive correlation with extreme precipitation events, whereas *L. gmelinii* was negatively correlated with extreme precipitation events. On an annual scale (**Fig. 4**), *P. sylvestris* showed a highly significant negative correlation with TXx and a positive correlation with R10 and precipitation. In contrast, *L. gmelinii* showed a highly significant negative correlation only with R99P.

On a monthly scale (**Fig. 5**), *P. sylvestris* showed a strong correlation with extreme warming indices, and the response had a certain lag effect. *L. gmelinii* showed a strong correlation with extreme cold indices. *P. sylvestris* showed a strong negative correlation with TXx ($r = -0.415$, $p < 0.01$) in October of the previous year, with TXx ($r = -0.442$, $p < 0.01$) and TX90P ($r = -0.463$, $p < 0.01$) in June

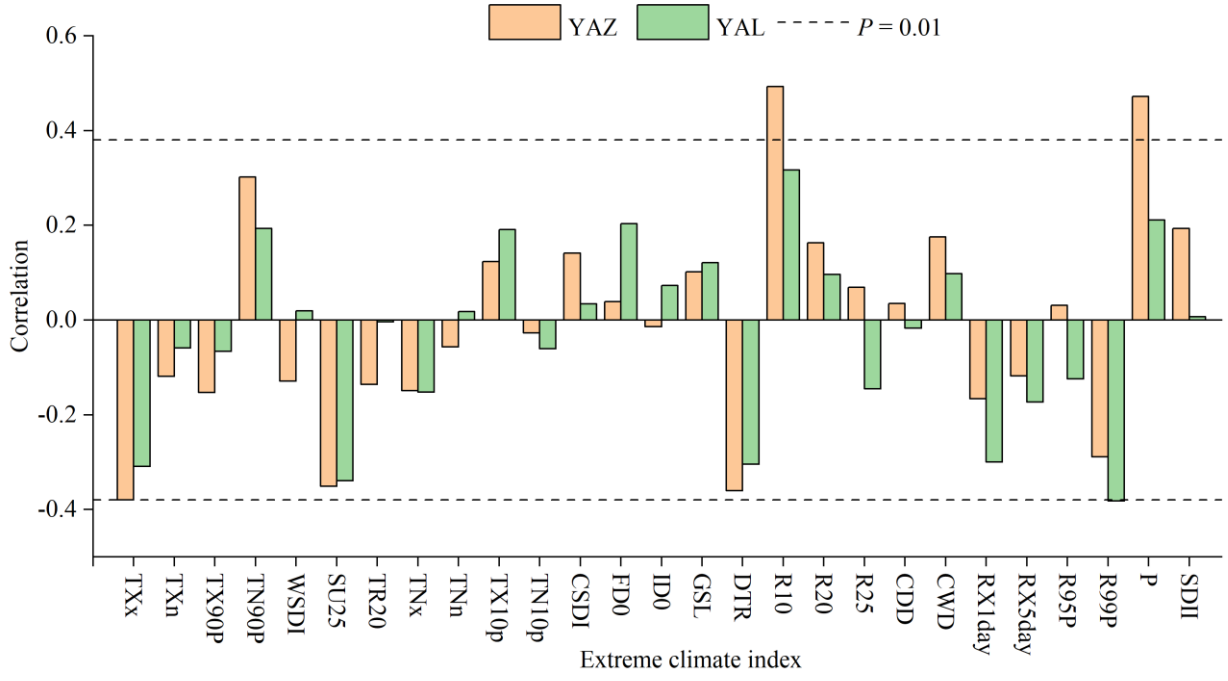

Fig. 4. *Correlation between annual extreme climate indices and the standard chronologies of* P. sylvestris *(YAZ) and* L. gmelinii *(YAL) dotted line: P = 0.01.*

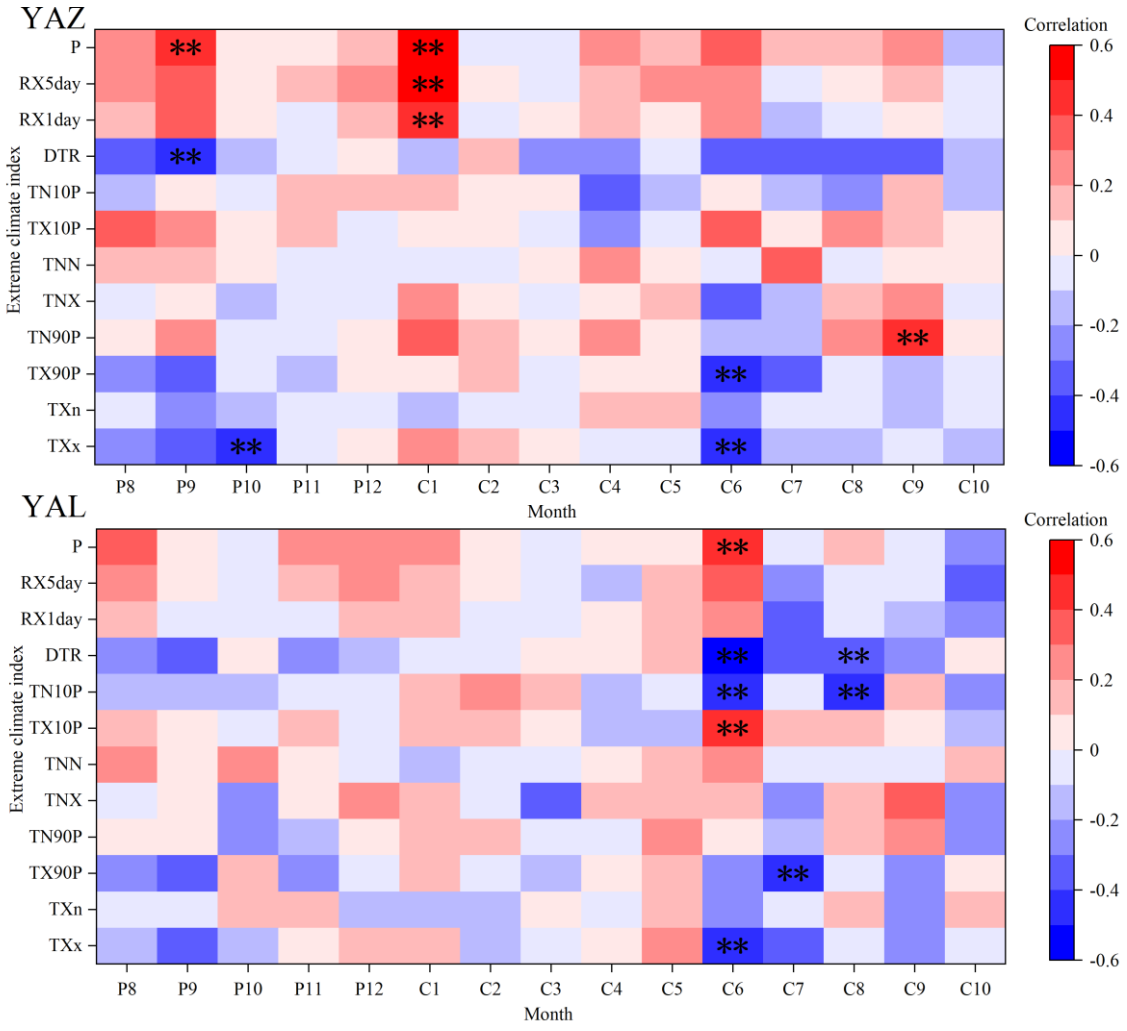

Fig. 5. *Correlation between monthly extreme climate indices and the standard chronologies of* P. sylvestris *(YAZ) and* L. gmelinii *(YAL). ** denotes: P < 0.01.*

of the current year, and a highly significant positive correlation with TN90P (r = 0.423, p < 0.01) in September of the current year. However, the correlation with extreme cold indices did not reach a level of significance higher than 0.01. The radial growth of *L. gmelinii* was significantly and negatively correlated with TXx (r = −0.415, p < 0.01) in June, TX90P (r = −0.406, p < 0.01) in July, TN10P (r_C6 = −0.446, r_C8 = −0.427, p < 0.01), and DTR (r_C6 = −0.525, r_C8 = −0.384, p < 0.01) in June and August of the current year. *P. sylvestris* exhibited a stronger response to extreme precipitation and showed a highly significant positive correlation with RX1day (r = 0.443, p < 0.01), RX5day (r = 0.527, p < 0.01), and precipitation (r = 0.534, p < 0.01) in January and was positively correlated with precipitation (r = 0.434, p < 0.01) in September of the previous year. Only *L. gmelinii* showed a highly significant positive correlation with precipitation (r = 0.400, p < 0.01) during June of the current year.

3.4 Fitting results of the tree-ring width chronology

When fitting the radial growth for the two tree species, only 12 monthly extreme climate factors (TXx, TXn, TX90p, TN90p, TNx, TNn, TX10p, TN10p, DTR, RX1day, RX5day, and P) totalling 180 extremes were used in the model, because the correlation between radial growth of the two species and monthly extreme climatic factors was more significant. Overall, the growth simulation of *P. sylvestris* was superior.

From the results of the *P. sylvestris* growth simulation obtained from the fitting (**Fig. 6a**), it can be seen that the 14 climatic factors screened were TXx_P10, TXx_C6, TX90P_C6, TN90P_C1, TNX_C6, TNn_C7, TX10P_P8, TN10P_C9, DTR_P9, DTR_C7, and DTR_C8, extreme precipitation, RX5day_C1, p_P9, and p_C1. The regression equation is shown in **Table 4**. On the basis of the cross-validation test proposed achieved optimal (**Table 4**, λ = 0.037), the R^2 of the regression model was 0.698, the

Table 4. *Lasso Regression equations of* P. sylvestris *and* L. gmelinii.

Species	Lasso Regression equation
P.sylvestris	Y=1.474 - 0.006 × (TXx_P10) - 0.007 × (TXx_C6) -0.003 × (TX90P_C6) + 0.001 × (TN90P_C1) - 0.001 × (TNX_C6) + 0.017 × (TNn_C7) + 0.002 × (TX10P_P8) + 0.001 × (TN10P_C9) - 0.014 × (DTR_P9) -0.008 × (DTR_C7)-0.002 × (DTR_C8) + 0.015 × (RX5day_C1) + 0.001 × (p_P9) + 0.013 × (p_C1)
L. gmelinii	Y= 1.663 - 0.003 × (TXx_C6) - 0.008 × (TXn_C9) - 0.002 × (TX90P_P9) - 0.001 × (TX90P_C7) - 0.008 × (TNX_C3) - 0.003 × (TN10P_C6) - 0.002 × (TN10P_C8) - 0.001 × (DTR_P9) + 0.028 × (DTR_C6) - 0.001 × (RX1day_C7) + 0.0003 × (p_P8) + 0.004 × (p_C1)

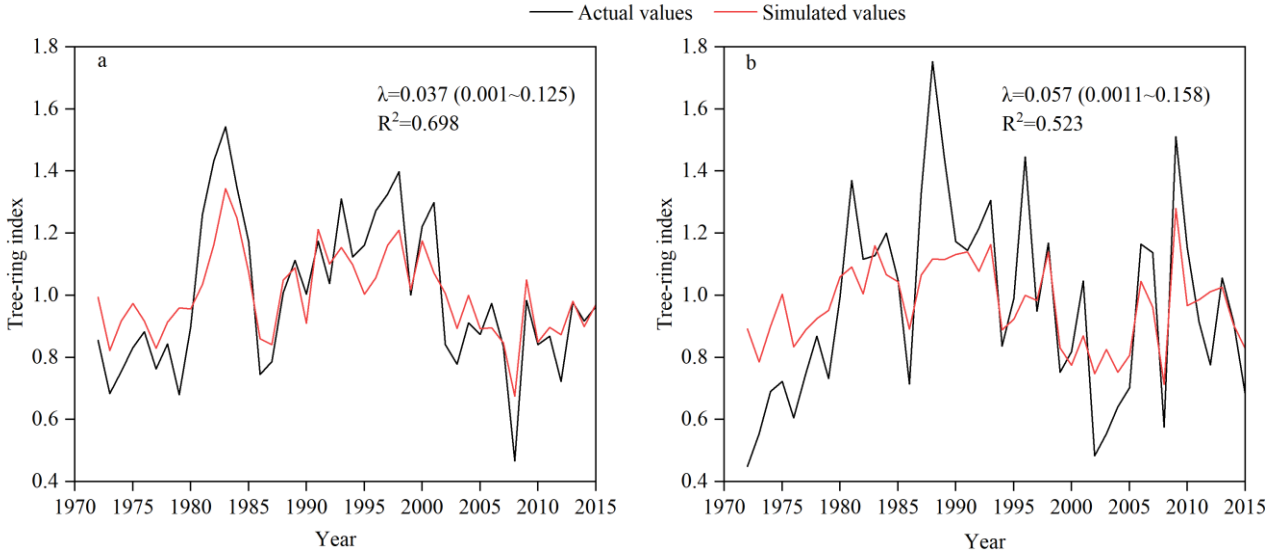

Fig. 6. *Model fitting results of* P. sylvestris *(a) and* L. gmelinii *(b) from 1972–2015.*

correlation coefficient between the fitted chronology and the original standard chronology was 0.898 ($p < 0.01$), and the MSE of the model was 0.019.

The radial growth trend of *L. gmelinii* was fitted (**Fig. 6b**) and 12 climatic factors were retained. The regression equations and validation parameters are listed in **Tables 4** and **5**, respectively. The results of the equation and each validation parameter showed that the tree-ring width of *P. sylvestris* fitted well, probably because its radial growth responded more closely to climate. When testing whether the relationship between tree growth and extreme climate indices selected by the LASSO regression changed over time (1972–2015), the relationship was found to be stable, indicating that it was possible to project climate-induced radial tree growth as demonstrated in this study (**Fig. 7**).

Table 5. *Lasso regression model parameters of P. sylvestris and L. gmelinii.*

Species	λ and recommended range	MSE	R^2	R
P.sylvestris	0.037 (0.001~0.125)	0.019	0.698	0.898
L. gmelinii	0.057 (0.0011~0.158)	0.031	0.523	0.819

3.5 Prediction of radial growth for the two tree species

The *P. sylvestris* and *L. gmelinii* responses to various extreme climate indices, and those obtained from fitting the standardized chronologies of the two species using the LASSO regression model, were combined with the climate prediction data for the SSP2-4.5 emission concentration scenario in the CMIP6 dataset to project the radial growth of the two species for the years 2015–2100. We defined the abnormal years as those in which values in the predicted series > mean + 1.5 SD (standard deviation) values < mean −1.5 SD, while those in the predicted series > mean + 2.5 SD and values < mean −2.5 SD were extreme anomaly years. Values in between were considered normal.

The projections obtained (**Fig. 8**) indicated that from 2015 to 2100, the result of fitting the predicted growth series of *P. sylvestris* showed a decreasing trend of −0.03 per decade. However, the changing trend of *L. gmelinii* growth was not significant. The mean value of the predicted growth series of *P. sylvestris* was 0.814, with an SD of 0.126, as shown in **Fig. 9a**. Three abnormally high values (2020, 2033, and 2036), six abnormally low values (2077, 2081, 2085, 2086, 2090, and 2093), and one extremely abnormally low value (2073) occurred in the

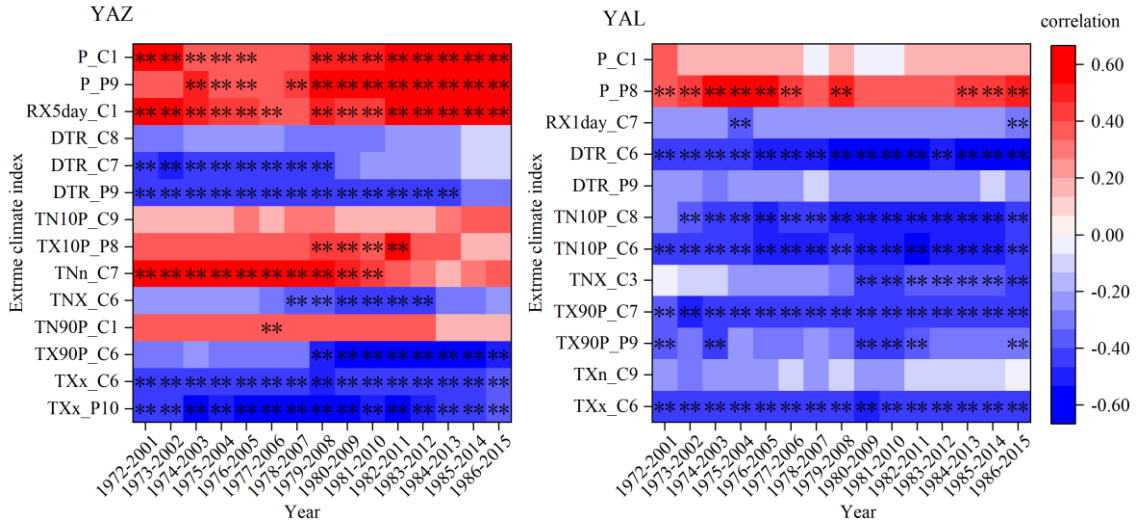

Fig. 7. *Moving correlation analysis of standard chronologies with extreme climatic indices. ** denotes: P < 0.01*

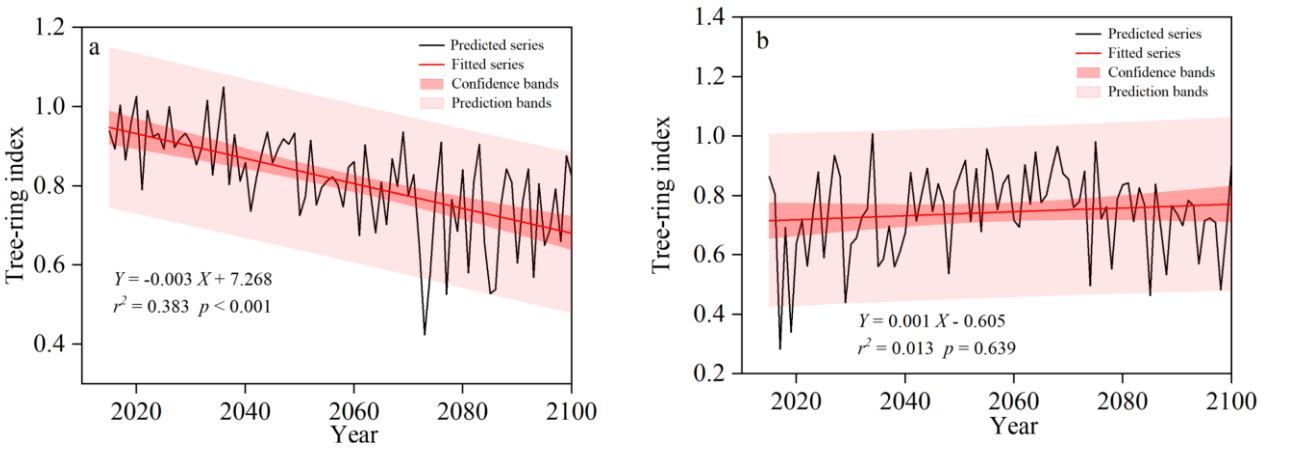

Fig. 8. *Growth prediction of* P.sylvestris *(a) and* L. gmelinii *(b) under SSP2-4.5 emission concentration scenario from 2015-2100. The black line represents the predicted series, the red line is the fitted series, and the shaded region represents the 95% confidence bands and prediction bands.*

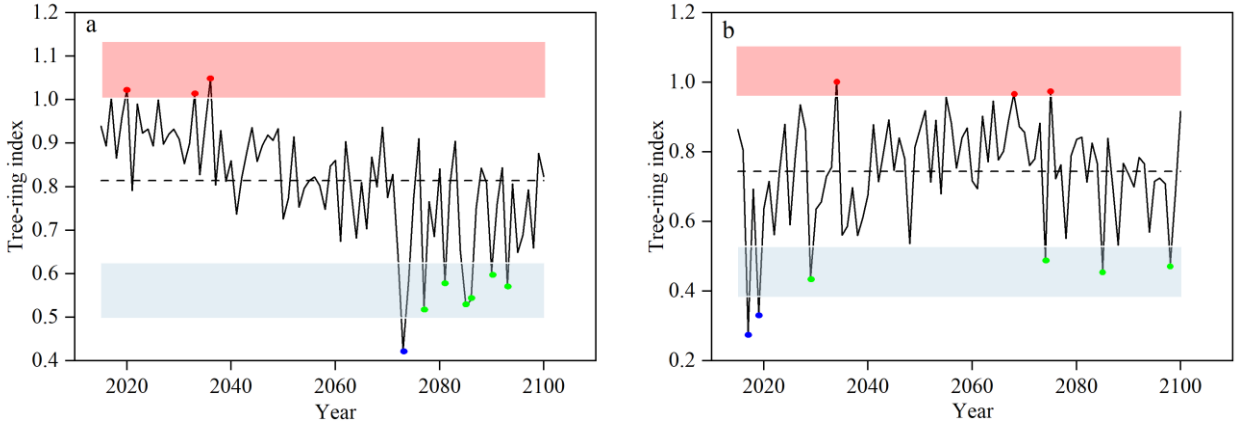

Fig. 9. *The growth trend and characteristics of* P.sylvestris *(a) and* L. gmelinii *(b) under the SSP2-4.5 emission concentration scenario. Red area: 1.5*SD < y <2.5*SD; Blue area: -2.5*SD < y <-1.5*SD; Red spot represents abnormally high value, green spot represents abnormally low value, and blue spot is extremely abnormally low value.*

2015–2100 period. The predicted growth series of *L. gmelinii* (**Fig. 9b**) had a mean value of 0.744 and an SD of 0.144. Two extremely abnormally low values (2017, 2019), four abnormally low values (2029, 2074, 2085, and 2098), and tree abnormally high values (2034, 2068, and 2075) occurred. Both tree species had more years with abnormally low values than those with abnormally high values, probably because extreme high temperatures inhibited tree growth in the region.

4. Discussion

4.1 Driving mechanism of extreme climate

The Daxing'anling Mountains are vulnerable to extreme climate events and their ecosystems are highly responsive to global warming (Jiang *et al.*, 2016; Zhao *et al.*, 2016). In this study, we found that, over the last 43 years, there was a significant increase in the extreme warm index, a decrease in the extreme cold index, and no significant trend in extreme precipitation. Similar changes in extreme climate indices have been observed in other regions (Choi *et al.*, 2009; Guo *et al.*, 2019; Ying *et al.*, 2020), and changes in atmospheric circulation patterns are dynamically linked to the probability of occurrence of extreme events (Horton *et al.*, 2015). Particularly, Zhuang *et al.* (2018) reported that consistent warming in northeast China corresponded to an 850 hPa anticyclonic anomaly; thus, we analyzed the variation in geopotential height and wind fields at 850 hPa in this study area. The 850 hPa geophysical height trend (**Fig. 10a**) analysis showed that positive anomalies over the entire Northeast region and exceeded the 95% confidence test. These anomalies weakened the meridional circulation in East Asia and were not conducive to the occurrence of cold air in the north of northeast China moving southward with the post-trough northwest airflow. Moreover, the northerly location of the westerly jet stream was not conducive to the southward intrusion of cold polar air (**Fig. 10b**), which can easily lead to higher overall temperatures in northeast China. In general, the influence of atmospheric circulation on extreme events in northeast China is relatively complex. Therefore, future studies should conduct multi-scale analyses of extreme events.

4.2 Effect of extreme climate change on tree-ring growth

The tree-ring chronologies of the two species were negatively correlated with annual extreme warm temperature indices. This finding suggests that continued climate warming may have reduced the radial growth of trees in this region. A strong negative correlation was observed between TXx and TX90P in June and July. This inverse relationship may be attributed to the increased transpiration and reduced soil moisture during high-temperature conditions. Simultaneously, the adverse effects of elevated temperatures on plant physiological processes during the growing season likely contributed to the slowdown in tree growth. It is generally accepted that 10–15°C above ambient temperature causes leaf damage and accelerates tree mortality (Kitudom *et al.*, 2022). Extreme high-temperature stress reduces the light energy use efficiency of photosynthetic organelles by reducing stomatal conductance and the net photosynthetic rate (Sun *et al.*, 2007), and ultimately reducing tree growth. Also, high-temperature-induced oxidative stress in plant leaves is also an important primary cause of oxidative damage (Chakraborty and Pradhan, 2011).

Extremely high temperature events often lead to drought and exacerbate tree growth stress by reducing precipitation and increasing the saturated water pressure deficit. In this study, we found that the extreme warm index increased significantly, whereas extreme precipitation did not. With increased frequency and intensity of extreme thermal events in Daxing'anling, the evaporation of surface moisture is likely to accelerate, along with insufficient precipitation to meet the water needs of the vegetation and

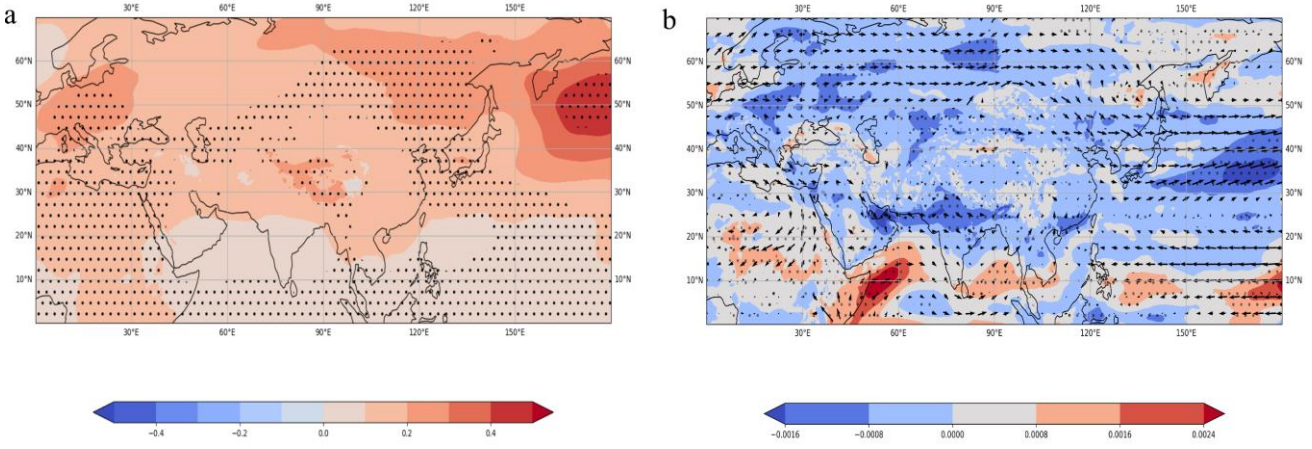

Fig. 10. *Trends of (a) geopotential height and (b) wind speed at 850 hPa during 1972–2015. Black spot: p < 0.01; Red areas represent upward trends, blue areas represent downward trends.*

soil, resulting in increased drought in the study area. Carbon starvation can occur when non-structural carbohydrates are depleted due to stomatal closure and reduced carbon assimilation during extended drought. Hydraulic failure can also occur because of xylem dysfunction caused by runaway embolisms. (Gentine *et al.*, 2016). In this study, the growth of *P. sylvestris* and *L. gmelinii* was positively correlated with the monthly extreme precipitation indices, indicating that increased precipitation extremes may reduce the impact of drought on tree growth during continued climate warming. Overall, extreme droughts caused by extremely warm conditions and low precipitation are likely to be the main factors hindering tree growth.

Differences in the effects of climate change on the growth of different tree species in the same habitat have been previously reported in the Daxing'anling Mountains (Sumaira *et al.*, 2019; Yang *et al.*, 2021), however, differences in tree growth responses to extreme climate indices need to be further studied. In this study, we found that the tree-ring widths of *P. sylvestris* and *L. gmelinii* differed in their responses to extreme climate indices. *P. sylvestris* responded more significantly to extremely high temperature indices and precipitation, with a certain lag effect. In contrast, *L. gmelinii* responded significantly to the extreme cold temperature indices. Compared with the drought- and barren-soil-tolerant *L. gmelinii*, *P. sylvestris* prefers moist and rich growing conditions (Xu, 1998). Therefore, *P. sylvestris* is more susceptible to climate change during significantly higher temperatures and frequencies of extreme weather events such as drought and frost. In addition, *P. sylvestris* is a shallow-rooted species; its water storage capacity and ability to access deep soil water resources are limited, and it is more susceptible to drought and precipitation during its growing period. However, *P. sylvestris* was highly significantly and positively correlated with TN90P in September, suggesting that with an increase in night-time temperature and sufficient night accumulation, the vegetation could be protected from extremely low temperatures, which is beneficial for vegetation growth. The *P. sylvestris* growth response to extreme temperatures had an obvious lag effect, which may reflect that tree growth feedback to the temperature needs a certain time to develop, probably due to the influence of soil temperature changes and the soil organic matter decomposition process. *P. sylvestris* is a species with perennial foliage and biennial cones. Thus, its physiological growth rhythm is different from that of *L. gmelinii*, where the cones ripen in September and the leaves fall in winter (Larcher, 1995). *L. gmelinii* was negatively correlated with TN10P in June and August, and positively correlated with TX10P in June. *L. gmelinii* is a light-loving, extremely cold-tolerant but heat-intolerant species that stops growing when the temperature exceeds 28°C. Therefore, higher daytime temperatures are not suitable for its growth. *L. gmelinii* is capable of physiological activity in cold soils, completing its life cycle through intense assimilation and transpiration within a short growth period. The characteristics of winter leaf shedding contribute to strong cold resistance (Zhou *et al.*, 1997). Therefore, the correlation with extremely low temperatures was more significant. Overall, tree species specificity may be why the two species exhibit different growth–climate relationships, which makes it imperative for us to accurately predict the trends and growth characteristics of tree species against the background of complex changes in extreme climate.

4.3 Analysis of predicted changes in tree-ring growth

Climate projections suggest that multiple extreme events (e.g., severe warming and drought) may be more likely than one event alone (Sillmann and Roeckner, 2007). This poses a significant threat to the functioning of forest ecosystems. Analyses of future climate change on the Qinghai–Tibetan Plateau revealed a general lengthening of the growing season for trees, which could have a significant impact on carbon sequestration in the region (He *et al.*, 2018). Predictions for different tree species in Finland using the CMIP5 model showed that climate change may primarily increase *P. sylvestris L.* growth, whereas *Picea abies L.* growth in the south may decrease significantly (Kellomäki *et al.*, 2018). Future climate change in Daxing'anling will be more extreme, and more severe and frequent extreme events, such as high temperatures and droughts, will pose a greater challenge to tree growth. *P. sylvestris* showed a marked decline in 2020–2100, whereas the change in *L. gmelinii* was not significant. However, when viewed in the two segments, there was a significant downward trend in *L. gmelinii* growth in the period 2075–2100, and both species had extremely low values in the late period. To investigate the reasons for the differences in growth responses under current and future extreme climatic conditions, this study conducted a linear regression trend analysis on the CMIP6-predicted extreme climate indices from 2015 to 2100, which were significantly associated with the growth response of two tree species based on Lasso regression analysis (**Fig. 11**). The results revealed that from 2015 to 2100, the study area's extremely high temperature indices exhibited a significant upward trend, while the tree-ring width for the two species showed a significant negative correlation with the extremely high temperature indices, indicating that the future increase in high temperature could negatively affect the growth of the two tree species. Furthermore, the cold indices significantly negatively correlated with the *L. gmelinii* exhibited a downward trend in the future, which might partially offset the impact of the increasing high temperature indices on its growth, leading to a less pronounced change in the *L. gmelinii* compared to the *P. sylvestris*. The changes in extreme precipitation indices were not significant, suggesting that future variations in precipitation levels might not have a noticeable impact on the growth of the two tree species. In addition, *P. sylvestris* is an evergreen conifer species that still respires in winter and, therefore, responds to climatic environmental factors for a longer period. Based

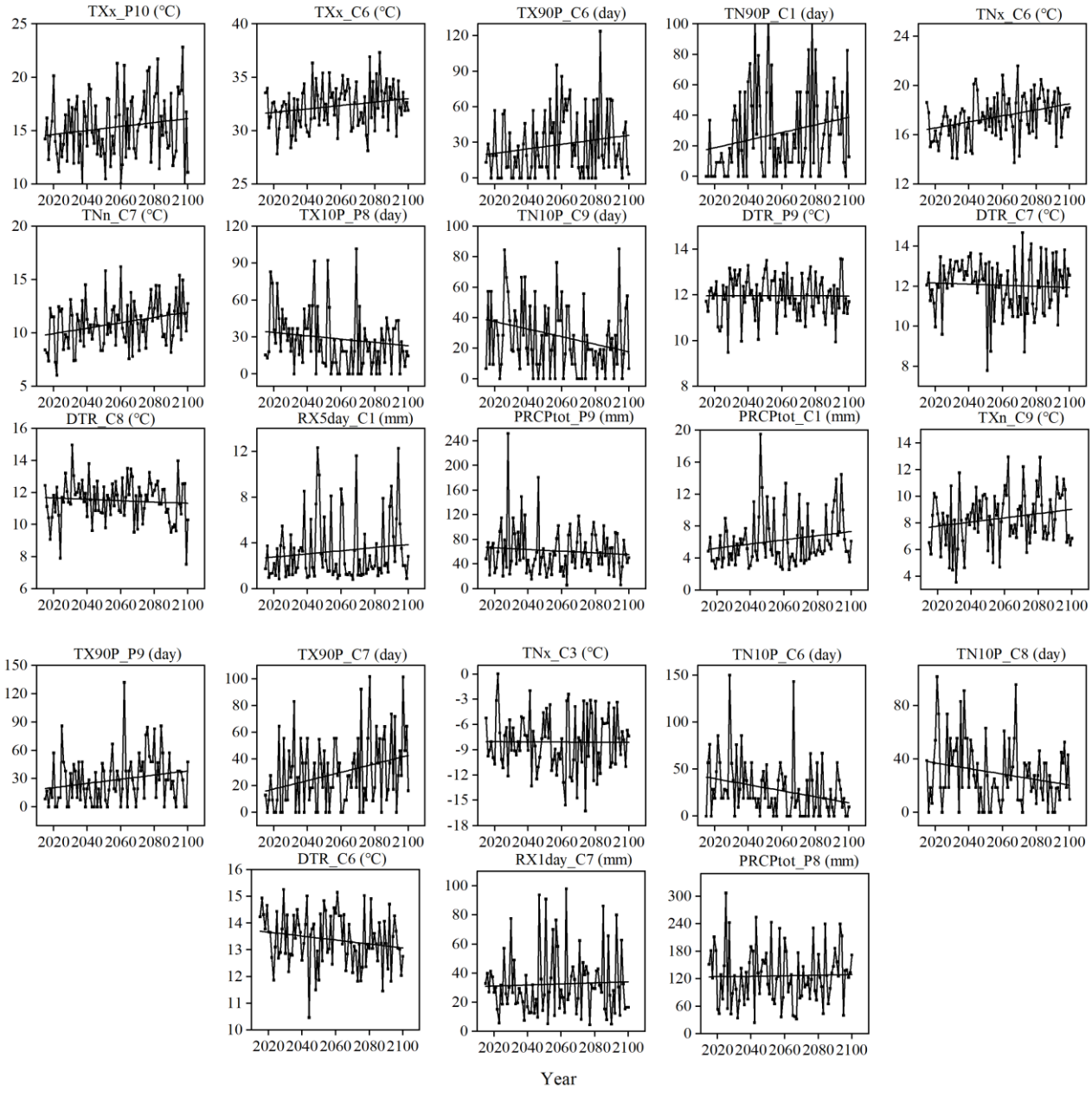

Fig. 11. *Variation trends of extreme climate during 2015–2100.*

on the responses analyzed above, we showed that the growth of *P. sylvestris* responded more strongly to extreme warmth and precipitation indices and may be more responsive during episodic climatic events, such as high temperature, drought, and frost; therefore, growth will be more obviously restricted, and its decline will be more pronounced in the future. *L. gmelinii* occurs in deep soils and has a greater ability to access groundwater. When water shortages are accompanied by increased temperatures, plant adaptation may be enhanced, but further increases in the intensity or frequency of droughts as moisture conditions continue to change may complicate the results (Yan *et al.*, 2023).

It should be noted that the CMIP6 model used to predict the changes in growth of the two tree species from 2020 to 2100 was improved in terms of the number of models, structure, and parameterization compared with previous versions; however, further refinement of the model adaptations based on the study area is required by the research teams. The LASSO regression model can solve the problem of multicollinearity and, for high-dimensional datasets, it can automatically perform feature

selection, which helps reduce the risk of overfitting. However, when there is a high degree of correlation between data features, LASSO regression tends to select one of the features and discard the other highly correlated features. The CMIP6 data provided a better fit for *P. sylvestris* growth, but a poorer fit for *L. gmelinii*, which may also affect the future trends of the dominant climatic factors for both species, and thus, the prediction of future growth trends for both species. Nevertheless, the results of this study are essential for understanding the responses of different tree species to climatic extremes. Our results provide valuable insights into targeted conservation and management strategies in the face of future climate change.

5. Conclusions

Over the past 44 years, extreme warm temperature events have increased in frequency, while the probability of extreme cold temperature events have decreased north of Daxing'anling. The weakening of the East Asian meridional circulation and the northward drift of westerly rapids may jointly result in changes in extreme climate events. A comparison of the radial growth of *P. sylvestris* and *L. gmelinii* under extreme climatic conditions indicated that extreme drought caused by extremely warm conditions and low precipitation is likely to be the main factor hindering tree growth. Using the CMIP6 model results and the LASSO model, we predicted the radial growth of the two species under various SSP2-4.5 emission scenarios using extreme climate indices. Our results showed a significant decrease in *P. sylvestris* growth, whereas the effect on *L. gmelinii* growth was not significant although it may also decrease slightly during severe climate change. Both tree species had more years with abnormally low tree-ring width values than years with abnormally high values in 2015–2100. Therefore, forest degradation is a challenge that this region will continue to face in the long term.

Acknowledgments

The research was supported by the Scientific and Technological Development Fund of Urumqi Institute of Desert Meteorology, China Meteorological Administration (Urumqi Institute of Desert Meteorology, China Meteorological Administration, KJFZ202306) "Reconstruction of Historical Runoff of Rivers in the Circum-Tarim Basin Based on Tree-Rotor Data, Estimation of Future Trends and Response Research";

China Desert Weather Scientific Research Fund (Urumqi Institute of Desert Meteorology, China Meteorological Administration, Sqj2023003) "Response of radial growth of different tree species to climate extremes and its future growth prediction in the eastern Tianshan Mountains". Outstanding Youth Science Fund of Natural Science Foundation of Xinjiang Uygur Autonomous Region (2022D01E105) "Research on Tree Ring Change and Climate Influence Mechanism of Major Conifer Species in Xinjiang and its Surrounding Areas"; Intergovernmental Key Programmes of the National Key R&D Programmes (Ministry of Science and Technology of the People's Republic of China, 2023YFE0102700) "Study on the Facts of Climate and Hydrological Changes in the Pamir Plateau in the Past Millennium and Future Projections and Responses"; Natural Science Foundation of China (41975095) "Multiple Tree-ring Parameters Based Stability Study of Climatic Response Under the Context of Global Change and Climate Reconstruction for Central Asia". Particular thanks are extended to the anonymous reviewers and editors whose comments and suggestions helped us greatly in improving this manuscript. We thank Leonie Seabrook, PhD, from Liwen Bianji (Edanz) (www.liwenbianji.cn), for editing the English text of a draft of this manuscript.

References

Ali S, Eum HI, Cho J, Li D, Khan F, Dairaku K, Koji Dairaku, Shrestha ML, Hwang S, Nasim W, Khan AI and Fahad S, 2019. Assessment of climate extremes in future projections downscaled by multiple statistical downscaling methods over Pakistan. *Atmospheric research* 222: 114–133, DOI 10.1016/j.atmosres.2019.02.009.

Allen CD, Macalady AK, Chenchouni H, Bachelet D and McDowell NG, 2010. A global overview of drought and heat-induced tree mortality reveals emerging climate change risks for forests. *Forest Ecology and Management* 259(4): 660–684, DOI 10.1016/j.foreco.2009.09.001.

Bonsal BR, Zhang X, Vincent LA and Hogg WD, 2001. Characteristics of Daily and Extreme Temperatures over Canada. *Journal of Climate* 14(9): 1959–1976, DOI 10.1175/1520-0442(2001)014<1959:CODAET>2.0.CO;2.

Chakraborty U and Pradhan D, 2011. High temperature-induced oxidative stress inLens culinaris, role of antioxidants and amelioration of stress by chemical pre-treatments. *Journal of Plant Interactions* 6(1): 43–52, DOI 10.1080/17429145.2010.513484.

Chen H, Sun J, Lin W and Xu H, 2020. Comparison of CMIP6 and CMIP5 models in simulating climate extremes. *Science Bulletin* 65(17): 1415–1418, DOI 10.1016/j.scib.2020.05.015.

Choi G, Collins DJ, Ren GY, Trewin B, Baldi M, Fukuda Y, Afzaal M, Pianmana T and Purevjav G, 2009. Changes in means and extreme events of temperature and precipitation in the Asia-Pacific Network region, 1955–2007. *International Journal of Climatology* 29(13): 1906–1925, DOI 10.1111/gcb.13973.

Ciais P, Reichstein M, Viovy N, Granier N, Ogée J, Allard V, Aubinet M, Buchmann N, Bernhofer C, Carrara A, Chevallier F, De Noblet N, Friend AD, Friedlingstein P, Grünwald T, Heinesch B, Keronen P, Knohl A, Krinner G, Loustau D, Manca G, Matteucci G, Miglietta F, Ourcival JM, Papale D, Pilegaard K, Rambal S, Seufert G, Soussana JF, Sanz MJ, Schulze ED, Vesala T and Valentini R, 2005. Europe-wide reduction in primary productivity caused by the heat and drought in 2003. *Nature* 437(7058): 529–533, DOI 10.1038/nature03972.

Cook ER, 1985. A time-series analysis approach to tree-ring standardization (Dendrochronology, forestry, dendroclimatology, autoregressive process). PhD dissertation. Tucson: The University of Arizona.

Dannenberg MP, 2021. Modeling tree radial growth in a warming climate: Where, when, and how much do potential evapotranspiration models matter? *Environmental Research Letters* 16(8): 084017, DOI 10.1088/1748-9326/ac1292.

Esper J and Schweingruber FH, 2004. Large-scale treeline changes recorded in Siberia. *Geophysical Research Letters* 31(6): L06202, DOI 10.1029/2003GL019178.

Fritts HC, 1976. Tree rings and climate. Kluwer Academic, New York.

Frost HR and Amos CI, 2017. Gene set selection via LASSO penalized regression (SLPR). *Nucleic Acids Research* 45(12): e114, DOI 10.1093/nar/gkx291.

Gao WF, Yao YL, Liang H, Song LL, Sheng HC, Cai TJ and Gao DW, 2019. Emissions of nitrous oxide from continuous permafrost region in the Daxing'an Mountains, Northeast China. *Atmospheric Environment* 198: 34–45, DOI 10.1016/j.atmosenv.2018.10.045.

Gentine P, Guérin M, Uriarte M, Mcdowell NG and Pockman WT, 2016. An allometry-based model of the survival strategies of hydraulic failure and carbon starvation. *Ecohydrology* 9(3): 529–546, DOI 10.1002/eco.1654.

Grissino-Mayer HD, 2001. Evaluating crossdating accuracy: a manual and tutorial for the computer program COFECHA.

Guo EL, Zhang JQ, Wang YF, Quan L, Zhang RJ, Zhang F and Zhou M, 2019. Spatiotemporal variations of extreme climate events in Northeast China during 1960–2014. *Ecological Indicators* 96: 669–683, DOI 10.1016/j.ecolind.2018.09.034.

He M, Yang B, Shishov V, Rossi S, Bräuning A, Ljungqvist FC and Grießinger J, 2018. Projections for the changes in growing season length of tree-ring formation on the Tibetan Plateau based on CMIP5 model simulations. *International Journal of Biometeorology* 62(4): 631–641, DOI 10.1007/s00484-017-1472-4.

He XM, Jiang C, Wang J and Wang XP, 2022. Comparison of CMIP6 and CMIP5 models performance in simulating temperature in Northeast China. *Chinese Journal of Geophysics* 65(11): 4194–4207 (Chinese with English abstract), DOI 10.6038/cjg2022P0455.

Holm JA, Medvigy DM, Smith B, Dukes JS, Beier C, Mishurov M, Xu XT, Lichstein JW, Allen CD, Larsen KS, Luo YQ, Ficken C, Pockman WT, Anderegg WRL and Rammig A, 2023. Exploring the impacts of unprecedented climate extremes on forestecosystems: hypotheses to guide modeling and experimental studies. *Biogeosciences* 20(11): 2117–2142, DOI 10.5194/bg-20-2117-2023.

Horton DE, Johnson NC, Singh D, Swain DL, Rajaratnam B and Diffenbaugh NS, 2015. Contribution of changes in atmospheric circulation patterns to extreme temperature trends. *Nature* 522(7557): 465–469, DOI 10.1038/nature14550.

IPCC, 2021. Climate change 2021: the physical science basis.

Izworska K, Muter E, Matulewski P and Zielonka T, 2023. Tree rings as an ecological indicator of the reaction of Swiss stone pine (*Pinus cembra L.*) to climate change and disturbance regime in the extreme environment of cliff forests. *Ecological Indicators* 148: 110102, DOI 10.1016/j.ecolind.2023.110102.

Jiang YW, Zhang JH, Han SJ, Chen ZJ, Setälä HK and Yu JH, 2016. Radial Growth Response of Larix gmelinii to Climate along a Latitudinal Gradient in the Greater Khingan Mountains, Northeastern China. *Forests* 7(12): 295–295, DOI 10.3390/f7120295.

Kitudom N, Fauset S, Zhou YY, Zhai F, Li MR and He MJ, 2022. Thermal safety margins of plant leaves across biomes under a heatwave. *Science of the Total Environment* 806(2): 150416, DOI 10.1016/j.scitotenv.2021.150416.

Kreyling J, Jentsch A and Beierkuhnlein C, 2011. Stochastic trajectories of succession initiated by extreme climatic events. *Ecology Letters* 14(8): 758–764, DOI 10.1111/j.1461-0248.2011.01637.x.

Kulha N, Honkaniemi JH, Barrere J, Brandl S, Cordonnier T, Korhonen KT, Kunstler G, Paul C, Reineking B and Peltoniemi M, 2023. Competition-induced tree mortality across Europe is driven by shade tolerance, proportion of conspecifics and drought. *Journal of Ecology* 111(10): 2310–2323, DOI 10.1111/1365-2745.14184.

Larcher W, 1995. Physiological Plant Ecology 3rd ed. Springer, New York, 414., DOI 10.1007/978-3-642-87851-0.

Leng WF, He HS, Bu RC and Hu YM, 2007. Sensitivity analysis of the impacts of climate change on the potential distribution of three larch (Larix) species in northeastern China. *Journal of Plant Ecology* 31(5): 825–833, DOI 10.17521/cjpe.2007.0104.

Li J, Chen D, Fu D, Shi J and Jiang M, 1993. Heilongjiang Forests. The Northeast Forestry University Press, Harbin.

Li XQ, Zhang LN, Zeng XM, Wang KY, Wang YB, Lu QQ and Liu XH, 2020. Different response of conifer and shrubs radial growth to climate in the middle Loess Plateau. *Acta Ecologica Sinica* 40(16): 5685–5697 (Chinese with English abstract).

O'Donnell AJ, Renton M, Allen KJ and Grierson PF, 2021. The role of extreme rain events in driving tree growth across a continental-scale climatic range in Australia. *Ecography* 44(7): 1086–1097, DOI 10.1111/ecog.05671.

Reichstein M, Ciais P, Papale D, Steven V and Zhao M, 2007. Reduction of ecosystem productivity and respiration during the European summer 2003 climate anomaly: a joint flux tower, remote sensing and modelling analysis. *Global Change Biology* 13(3): 634–651, DOI 10.1111/j.1365-2486.2006.01224.x.

Ribbing J, Nyberg J, Caster O and Jonsson EN, 2007. The lasso - a novel method for predictive covariate model building in nonlinear mixed effects models. *Journal of pharmacokinetics and pharmacodynamics* 34(4): 485–517, DOI 10.1007/s10928-007-9057-1.

Roshani SH, Kumar P, Masroor M, Rahaman MH, Rehman S, Ahmed R and Sahana M, 2022. Forest vulnerability to climate change: A review for future research framework. *Forests* 13(6): 917, DOI 10.3390/f13060917.

Sanginés de Cárcer P, Vitasse Y, Peñuelas J, Jassey VEJ, Buttler A and Signarbieux C, 2017. Vapor–pressure deficit and extreme climatic variables limit tree growth. *Global Change Biology* 24(3): 1108–1122, DOI 10.1111/gcb.13973.

Kellomäki S, Strandman H, Heinonen T, Asikainen A, Venäläinen A and Peltola H, 2018. Temporal and Spatial Change in Diameter Growth of Boreal Scots Pine, Norway Spruce, and Birch under Recent-Generation (CMIP5) Global Climate Model Projections for the 21st Century. *Forest* 9(3): 118, DOI 10.3390/f9030118.

Sillmann J and Roeckner E, 2007. Indices for extreme events in projections of anthropogenic climate change. Climatic Change 86 (1–2): 83–104, DOI 10.1007/s10584-007-9308-6.

Song Y, Sterck FJ, Zhou XQ, Liu Q, Kruijt B and Poorter L, 2022. Drought resilience of conifer species is driven by leaf lifespan but not by hydraulic traits. *New Phytologist* 235(3): 978–992, DOI 10.1111/nph.18177.

Sumaira Y, Wang XC, Zhao HY, Zhu LJ, Yuan DY and Li ZS, Zhang YD, Ahmad S and Han SJ, 2019. Contrasting climate-growth relationship between Larix gmelinii and Pinus sylvestris var. mongolica along a latitudinal gradient in Daxing'an Mountains, China. *Dendrochronologia* 58: 125645, DOI 10.1016/j.dendro.2019.125645.

Sun GH, Zeng XP, Liu XJ and Zhao P, 2007. Effects of moderate high-temperature stress on photosynthesis in three saplings of the constructive tree species of subtropical forest. *Acta Ecologica Sinica* 27(4): 1283–1290, DOI 10.1016/S1872-2032(07)60029-8.

Thackeray, Chad W, Hall A, Norris J and Chen D, 2022. Constraining the increased frequency of global precipitation extremes under warming. *Nature Climate Change* 12(5): 441–448, DOI 10.1038/s41558-022-01329-1.

Wang X, Wang Y and Lin Q, 2023. Assessing Global Landslide Casualty Risk Under Moderate Climate Change Based on Multiple GCM Projections. *International Journal of Disaster Risk Science* 14: 751–767, DOI 10.1007/s13753-023-00514-w.

Wang Y, Li HX, Wang HJ, Sun B and Chen HP, 2021. Evaluation of CMIP6 model simulations of extreme precipitation in China and

comparison with CMIP5. *Acta Meteorologica Sinica* 79(3): 369–386, DOI 10.11676/qxxb2021.031.

Wigley TML, Briffa KR and Jones PD, 1984. On the average value of correlated 2 time series, with applications in dendroclimatology and hydrometeorology. *Journal of Climate and Applied Meteorology* 23(2): 201–203, DOI 10.1175/1520-0450(1984)023<0201:OTAVOC>2.0.CO;2.

Xu HC, 1998. Daxing'an Mountains Forest, China. Beijing: Science Press.

Yan H, Sun YJ, Zhou WY and Liu BH, 2023. Distinctions in drought adaptability and growth decline of Larix gmelinii at different latitudes in Greater Khingan Mountains. *Acta Ecologica Sinica* 43(10): 3958–3970, DOI 10.5846/stxb202112283696.

Yang JJ, Zhang QL, Song WH, Zhuo X, Li ZS, Zhang YD and Wang XC, 2021. Response differences of radial growth of Larix gmelinii and Pinus sylvestris var. Mongolia to climate change in Daxing'an Mountains, Northeast China. *The journal of applied ecology* 29(3): 380–385.

Ying H, Zhang H, Zhao J, Shan Y, Zhang Z and Guo X, 2020. Effects of spring and summer extreme climate events on the autumn phenology of different vegetation types of Inner Mongolia, China, from 1982 to 2015. *Ecological Indicators* 111: 105974, DOI 10.1016/j.ecolind.2019.105974.

Zang C, Hartl-Meier C, Dittmar C, Rothe A and Menzel A, 2014. Patterns of drought tolerance in major European temperate forest trees: climatic drivers and levels of variability. *Global Change Biology* 20(12): 3767–3779, DOI 10.1111/gcb.12637.

Zhang X, Zhou YZ, Ji YH, Yu M, Li XY, Duan J, Wang Y, Gao J and Guo X, 2023a. Climate Factors Affect Above–Belowground Biomass Allocation in Broad-Leaved and Coniferous Forests by Regulating Soil Nutrients. *Plants* 12(23): 3926–3926, DOI 10.3390/plants12233926.

Zhang Y, Piao SL, Sun Y, Rogers BM, Li X, Lian X, Liu Z, Chen A and Peñuelas J, 2023b. Future reversal of warming-enhanced vegetation productivity in the Northern Hemisphere, EGU General Assembly, Vienna, Austria 24–28, DOI 10.5194/egusphere-egu23-3016.

Zhao HY, Gong LJ, Qu HH, Zhu H, Li XF and Zhao F, 2016. The climate change variations in the northern Greater Khingan Mountains during the past centuries. *Journal of Geographical Sciences* 26(5): 585–602, DOI 10.1007/s11442-016-1287-y.

Zhou YL, Zu YG and Yu D, 1997. Vegetation Geography in Northeast China. Science Press, Beijing, 446 (Chinese with English abstract).

Zhu HH, Jiang ZL and Li L, 2021. Projection of climate extremes in China, an incremental exercise from CMIP5 to CMIP6. *Science Bulletin* 66(24): 2528–2537, DOI 10.1016/j.scib.2021.07.026.

Zhuang YH, Zhang JY, Wang YH and WU LY, 2018. Variability of Warm Season Surface Air Temperature over Northeastern China and Its Relationships with Sea Surface Temperature and Large-scale Atmospheric Circulation Pattern. Climatic and Environmental Research 23(4): 479–492 (Chinese with English abstract).